AIAA JOURNAL
Vol. 42, No. 1, January 2004

Suppression of Pressure Loads in Cavity Flows

Lawrence S. Ukeiley,* Michael K. Ponton,† John M. Seiner,‡ and Bernard Jansen§
University of Mississippi, University, Mississippi 38655

The need to suppress dynamic-pressure loads in open cavities represents an important problem in many aeronautical applications. Many studies have been conducted using passive and active control techniques at the leading and trailing edges of cavities that have shown some success at reducing the dynamic-pressure levels in simulated weapons bays. In this work a leading-edge fence along with a cylindrical rod, suspended in the approaching boundary layer parallel to the leading edge of the cavity, was examined. The overall pressure levels along with the spectral distribution of the surface pressure in the cavity have been shown to be altered in a favorable manner by both of these devices. Suppressing the dynamic-pressure levels in the cavity was also found to alter the correlation between sensors along the floor cavity. Although it was found that both leading-edge devices lift the shear layer away from the cavity, the manner in which it is lifted appears to play an important role in the level of surface-pressure suppression.

Introduction

THE dynamics of open cavities represent an important and potentially dangerous problem in many aircraft applications. Weapons bays have typically driven the research on open cavities and have three significant problems associated with them: radiated noise away from the aircraft, the ability to release stores from the bay, and the high dynamic-pressure loads inside the cavity, which can harm stores or even the structure of the aircraft. It is this last aspect that is driving the current research, although it is important to understand the effects on all aspects of the cavity. Studying the aeroacoustic environment in weapons bays requires an understanding of many important fluid dynamic and acoustic phenomena. The dynamics of the shear layer formed above the cavity and how it interacts with the aft wall of the cavity play a crucial role in understanding resonating cavities. This interaction of the shear layer with the aft wall provides a source for a propagating wave that moves upstream in the cavity. Although it is known that this event is a source driving the resonant modes in the cavity, there is still more essential dynamics between the shear layer and the cavity that need to be understood so that the broadband pressure levels in the cavity can be reduced in addition to the tonal components.

The pressure loads inside of cavities have been studied since the 1950s with the work of Krishanmurty[1] and Roshko.[2] The study of Rossiter[3] helped to quantify the effects of different length-to-depth aspect ratios and is best known for developing a relationship that can be used to predict the frequencies of the resonant modes in open cavities. Throughout the 1970s many studies were conducted that helped to develop an understanding of cavity flows and further the concept of control to alter the flow to reduce the adverse effects of the flow originally introduced by Rossiter. A few of these studies are described next. The discussion of previous studies is not intended to be a comprehensive review but rather highlight some studies that are similar in character to the one being reported here.

Heller and Bliss[4] conducted an analytical and experimental program that studied cavities exposed to subsonic and supersonic freestream flows. In their study they postulated mechanisms of how the shear layer and freestream flow interact with the aft wall of the cavity and evaluated several concepts for suppressing the discrete tones such as slanting the aft wall. A water table was used to visualize the aforementioned interactions, and they claimed that the important mechanism is not necessarily the interaction of the shear layer with the aft wall but instead the freestream flow impinging on the aft wall when the shear layer enters the cavity. Recently, schlieren images of a cavity in transonic flow by Heller and Delfs[5] have been shown to verify the earlier proposed mechanisms. The study of Clark[6] examined several techniques for reducing the turbulence in the shear layer and altering the cavity bay geometry to reduce the dynamic-pressure loads. He found that a porous leading-edge fence served to reduce the pressure level further than other devices such as tangential blowing. He also found that over the limited Reynolds number and transonic Mach-number ranges studied there was little difference in his results. Shaw[7] conducted flight tests with instrumented cavities over a range of Mach numbers from 0.6 to 1.3 to evaluate leading-edge spoilers and slanted trailing edges. It was found that the combination of the leading-edge spoiler with slanted aft wall reduced the tonal pressure components measured in the cavity; however, the static pressure in the cavity was reduced.

The fairly recent renewed emphasis on developing a better understanding for cavity flows has been spurred on by the fact that current and future generations of stealth aircraft will have no external stores. Hence cavities might be exposed to diverse flight conditions. Dix and Butler[8] reported on a large database collected to further quantify the effect of cavity geometry and examine a variety of suppression devices. Their study showed that the rms pressure levels inside the cavity are not affected greatly by the Reynolds number and that leading-edge spoilers are most effective in subsonic and transonic flows, whereas they lose their effectiveness in supersonic flows. Parts of this database were examined further by Dix and Bauer,[9] who developed relationships for predicting the peak amplitude of the tonal components. The experimental studies of Kegerise et al.[10] and Cattafesta et al.[11] have used techniques to view the density variations of the various modes along with signal-processing techniques to show the evidence of mode switching between various Rossiter modes.

Most of the recent emphasis in cavity research has been to develop control methodologies for the cavity aeroacoustic environment. This has been spurred on by the work of Shaw and McGrath.[12] They reported that it seems feasible for active control techniques to be used on real aircraft instead of some of the current passive ones. Sarno and Franke[13] conducted experiments to evaluate the suppression

Presented as Paper 2002-0661 at the 40th AIAA Aerospace Science Meeting, Reno, NV, 14–17 January 2002; received 30 October 2002; accepted for publication 20 July 2003.

*Research Scientist and Research Assistant Professor of Mechanical Engineering, Jamie L. Whitten National Center for Physical Acoustics. Senior Member AIAA.

†Research Engineer, Jamie L. Whitten National Center for Physical Acoustics; currently Professor, School of Education, Regent University, Virginia Beach, VA 23464-9800. Senior Member AIAA.

‡Associate Director, Jamie L. Whitten National Center for Physical Acoustics. Associate Fellow AIAA.

§Research Engineer, Jamie L. Whitten National Center for Physical Acoustics. Member AIAA.

levels for static and oscillating fences along with pulsed and steady mass injection at the cavity leading edge. They found that a static fence at the leading edge supplied the greatest level of suppression. Shaw and Northcraft[14] used a pulsed blowing system and a straightforward optimization algorithm to reduce the tones and broadband levels. Studies by Williams et al.[15] have used a leading-edge bleed system with a controller to suppress tonal components. Cattafesta et al.[16] used an adaptive control algorithm with piezoelectric actuators. Stanek et al.[17] reported on the use of many different high-frequency devices at the leading edge of a cavity in transonic flow and have shown them to be effective.

The studies of McGrath and Shaw[18] and Smith et al.[19] have reported on the use of cylinders suspended in the approaching boundary layers as a means of suppressing the fluctuating surface-pressure loads inside the cavity. McGrath and Shaw reported the first evidence that the use of a cylinder in the approaching boundary layer could significantly reduce the fluctuating surface-pressure levels in the cavity. They postulated that the reductions were caused by the interaction of the shedding vortices off of the rod with the shear layer above the cavity. The study of Smith et al. was based on parameterizing the optimum cylinder geometry and location. They concluded that the cylinder should have a diameter approximately one-third of the approaching boundary-layer thickness and the top of the cylinder should be aligned with the top edge of boundary layer.

This manuscript presents results of a study to suppress pressure loads in an open cavity subject to both subsonic and supersonic freestream flows. The overall goal of the study is to develop a sufficient understanding of the dynamics of the cavity so that active control concepts can be used in the future. The suppression reported here is accomplished by passive leading-edge devices such as solid fences and cylindrical rods at various heights in the approaching boundary layer. This is not the first study to use the proposed devices for suppressing the pressure oscillations in open cavities (see experimental studies[18,19] and numerical studies[20,21]). However, it is felt that by understanding how these devices work one should be able to develop a better mechanism for reducing pressure loads that does not adversely affect other properties of cavities such as store release.

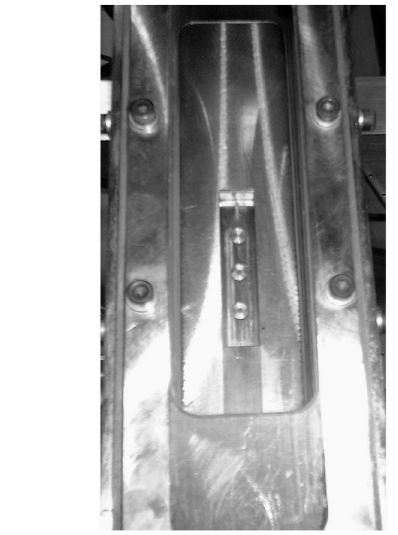

a) Cavity for subsonic studies

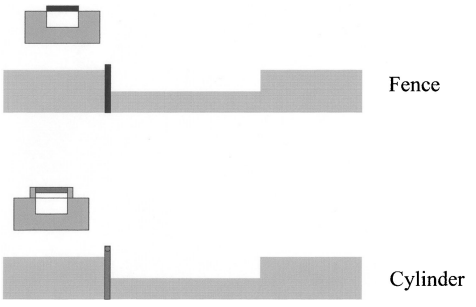

b) Geometry of leading edge devices

Fig. 1 Cavity duct in NCPA Anechoic Jet Laboratory and geometry of leading-edge devices.

Experimental Descriptions

Experiments were conducted in two facilities to study leading-edge devices designed for the suppression of pressure loads in open cavities. The experiments were conducted at Mach numbers of 0.6, 0.75, 0.8, and 1.4. In these experiments the spectral and correlation properties of the fluctuating surface pressures along the centerline of the cavity were measured. In addition, total pressure profiles at two streamwise locations were measured to evaluate the effect of the leading-edge devices on the shear layer above the cavity.

National Center for Physical Acoustics

The majority of the results acquired with subsonic freestream conditions, Mach 0.6 and 0.75, were acquired through experiments conducted in the Anechoic Jet Lab in the University of Mississippi's National Center for Physical Acoustics (NCPA). The facility has been described by Ponton et al.,[22] and only relevant details will be discussed here. The rectangular cavity studied was in the floor of a 254-mm-long duct with a 50.8×50.8 mm cross section. The flow entered the duct after being contracted from a 152.4-mm-diam plenum with a ceramic flow conditioning element. The freestream turbulence intensity in a nozzle of similar contraction to this facility was found to be 0.15%. The air delivery system consists of an Ingersol Rand Centac compressor and a Fisher Control valve controlled through PC-based LabView and allows the flow conditions to be held within 0.5% based on Mach number. The boundary layer at the leading edge of the cavity was measured to be approximately 2.54 and 2.03 mm for Mach 0.6 and 0.75, respectively. The unit Reynolds number in the duct was approximately 3.35×10^6 and 4.57×10^6 per meter for the Mach 0.6 and 0.75 cases, respectively. The cavity had a width of 14.22 mm and a depth of 7.11 mm. The length was configurable at 63.5 or 39.62 mm giving length to depth ratios of 9 and 5.6, respectively. The cavity had four locations for dynamic-pressure transducer insertion along the cavity centerlines axis. Three locations were on the bottom surface of the cavity at 15.88, 31.75, and 47.63 mm downstream of the cavity leading edge, and one location was in the center of the aft wall. Typically, only the two upstream floor-mounted sensors and the one in the aft wall were used. The dynamic pressure transducers used in this model were Kulite model XCW-093-5D, which are 2.36-mm-diam, 34.45-kPa differential sensors. The time-dependent pressures were digitized through a Unix-workstation-based data-acquisition system with an ICS 16 bit A/D converter capable of digitizing 32 channels simultaneously. For most cases the sensors were sampled at a rate of 250 kHz with 1,048,576 data points and were filtered at 100 kHz and 100 Hz for the low- and high-pass filters, respectively. This allowed for averaging of 256 blocks with a transform length of 4096 points. The total pressure measurements were averaged over 100 samples using a specially designed probe, which had a 0.13-mm hole exposed to the flow. Traversing of the probe for the inlet and shear-layer profiles was handled with a linear micrometer traverse, which allowed for the position being known within ± 0.01 mm. Figure 1a shows a picture of the cavity in the glass duct. Also visible in this picture is the total pressure probe at the leading edge of the cavity and the floor-mounted dynamic-pressure sensors. The cavity was designed so that the leading edge was removable and the suppression devices could be inserted. For the suppression studies reported here, either a solid fence was installed, or cylinders supported by rectangular posts were inserted at the leading edge of the cavity. Figure 1b shows the orientation of the leading-edge devices reported here.

U.S. Air Force Academy

The other sets of data analyzed in this manuscript were acquired through experiments conducted in the Trisonic Wind Tunnel at the

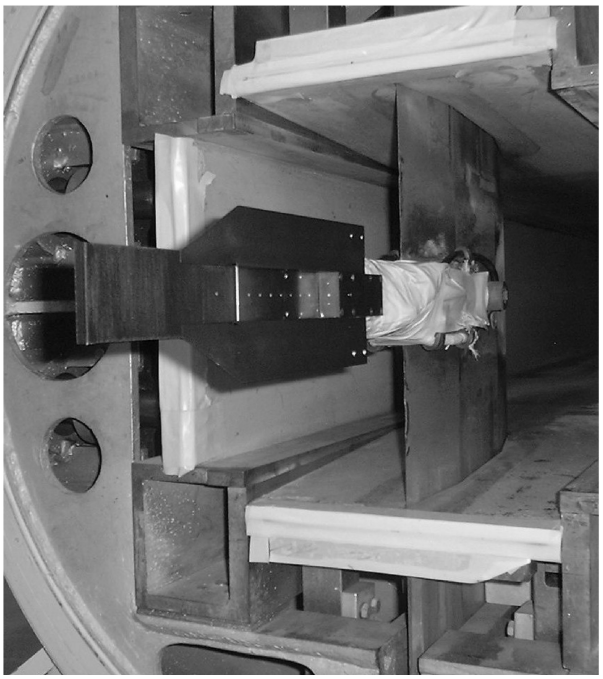

Fig. 2 Cavity in U.S. Air Force Academy Trisonic Tunnel.

U.S. Air Force Academy.[¶] It has several fixed Mach-number nozzle blocks and a 304.8×304.8 mm^2 test section. For the tests that will be discussed in this work, the tunnel was run at Mach 0.8 and 1.4, although only the supersonic cases will be discussed. The tunnel stagnation pressure was approximately 206.7 kPa, yielding a unit Reynolds number of 2.93×10^6 per meter and a dynamic pressure of 91 kPa. The model was sting mounted and had a blockage of 4% by area. A photograph of the model in the tunel is shown in Fig. 2. Tunnel unstart, for the supersonic case, was verified not to exist on the model by schlerien images and examining the static pressure on the model. The model used for these experiments was configurable for length-to-depth aspect ratios of 5.6 and 9 to match the experiments conducted in the NCPA. The physical dimensions of the cavity were twice that of the subsonic model, that is, a depth 14.22 mm, a width of 25.58 mm, and lengths of either 79.50 or 128.02 mm for the respective lift-to-drag (L/D) ratios. The model was instrumented with 13 pressure transducers along the centerline of the cavity. The sensors were Kulite model XCQ-062-25a, which have a 1.57-mm diam and are 172.28-kPa absolute pressure transducers. The same data-acquisition system as used for the experiments in the NCPA was used at the Air Force Academy. All of the sensors were sampled simultaneously in groups of 1,048,576 points at 250 kHz and filtered at 100 Hz and 100 kHz for the high- and low-pass filters, respectively. In addition, 16 static-pressure taps were used to monitor the mean static pressure and verify that there were no spanwise variations in the model. For the suppression studies with this model, posts that support a cylinder parallel to the leading edge of the cavity could be inserted. The posts were designed with sharp leading edges to minimize the effects of shocks.

Results

Discussion of the results will include examination of Mach-number profiles in the shear layer above the cavity as well as spectra, correlations, and integrated levels of the fluctuating surface pressure in the cavity for the subsonic and supersonic freestream conditions. They will be presented for cavity length-to-depth aspect ratios of 5.6 and 9.0. First, the results of the baseline cavity with no suppression elements will be discussed. Then the results with leading-edge suppression devices will be discussed and compared to the baseline cases in order to develop an understanding of the mechanisms used by these devices.

Baseline

In the following section experimental results of the baseline cavity will be discussed. The discussion of these results will include both aspect ratios at subsonic and supersonic Mach numbers. The results presented here agree quite well with much of the historic data and are presented to supply the background upon which the suppression results can be better understood.

Spectra

Narrowband spectra of open cavities have been reported in many studies, some of which were discussed in the Introduction, and are dominated by fairly high broadband levels and peaks with frequencies that can be reasonably well described by empirical and analytical relationships such as Rossiter's formula and the solution for normal modes. Figures 3–5 show comparisons of spectra obtained from the aft wall sensor and one of the sensors located in the cavity floor for both aspect ratios respectively and all three Mach numbers. In all plots the ordinate is the square root of the power spectral density (PSD) normalized by the dynamics pressure Q and the abscissa is frequency in hertz. Although the data were low-pass filtered at 100 kHz, these plots are truncated at 20 kHz so that the behavior at lower frequencies can clearly be seen. All of the spectral plots presented in this manuscript, before being normalized, have units

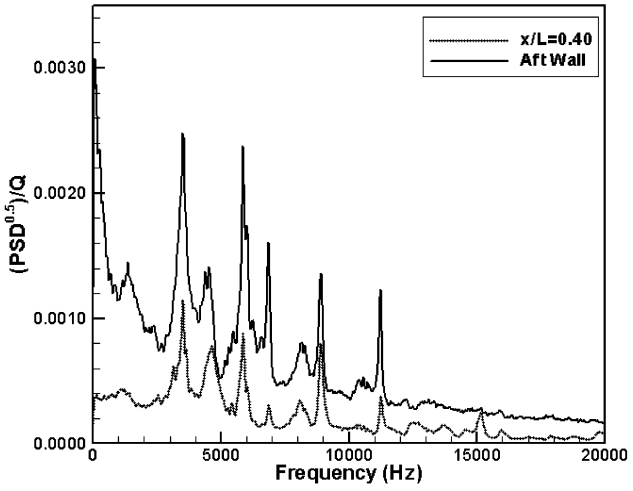

a) *L/D* = 5.6

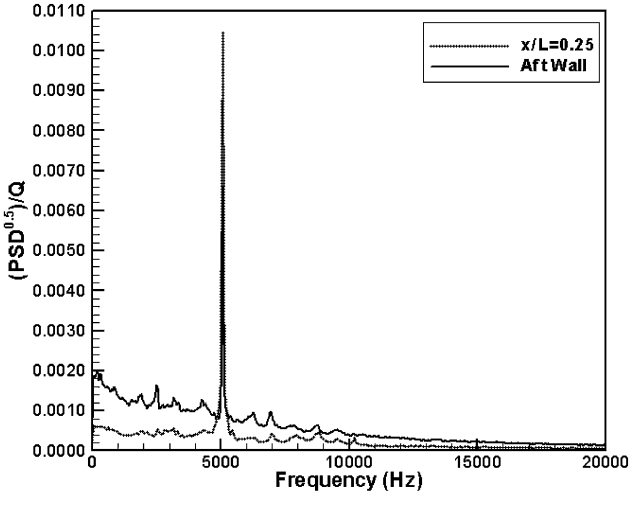

b) *L/D* = 9.0

Fig. 3 Baseline surface-pressure spectra for Mach 0.6 freestream condition.

[¶]Details of the Trisonic facility can be found on the Air Force Academy web page at http://www.usafa.af.mil/dfan/lab/trisonic.htm.

Table 1 Frequency of Rossiter modes

Mode number	Mach 0.6 $L/D=5.6$	Mach 0.6 $L/D=9.0$	Mach 0.75 $L/D=5.6$	Mach 0.75 $L/D=9.0$
1	1,588	991	1,819	1,135
2	3,706	2,312	4,245	2,649
3	5,823	3,634	6,670	4,162
4	7,941	4,954	9,095	5,676
5	10,058	6,276	11,521	7,189

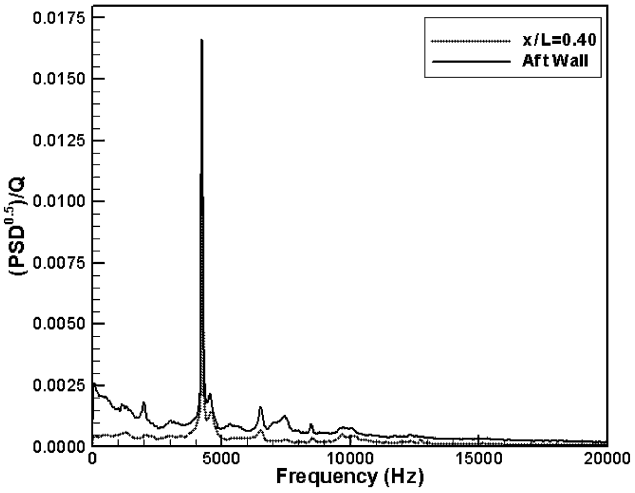

a) *L/D* = 5.6

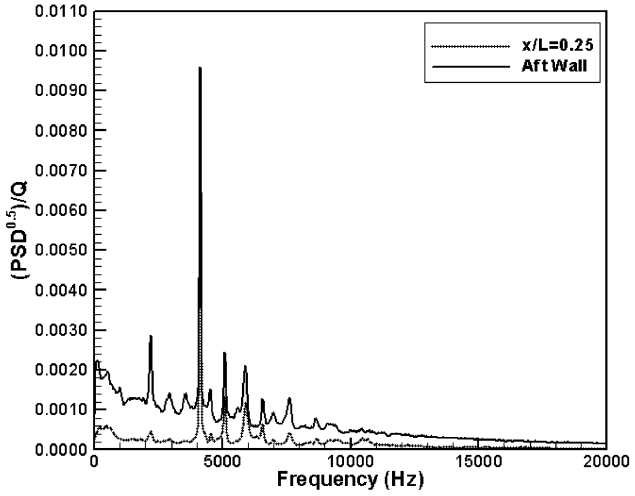

b) *L/D* = 9.0

Fig. 4 Baseline surface-pressure spectra for Mach 0.75 freestream condition.

Table 2 Frequency of longitudinal cavity modes

Mode number	Mach 0.6 $L/D=5.6$	Mach 0.6 $L/D=9.0$	Mach 0.75 $L/D=5.6$	Mach 0.75 $L/D=9.0$
1	4,192	2,616	4,116	2,568
2	8,384	5,231	8,232	5,137
3	12,576	7,847	12,348	7,705
4	16,768	10,463	16,464	10,273

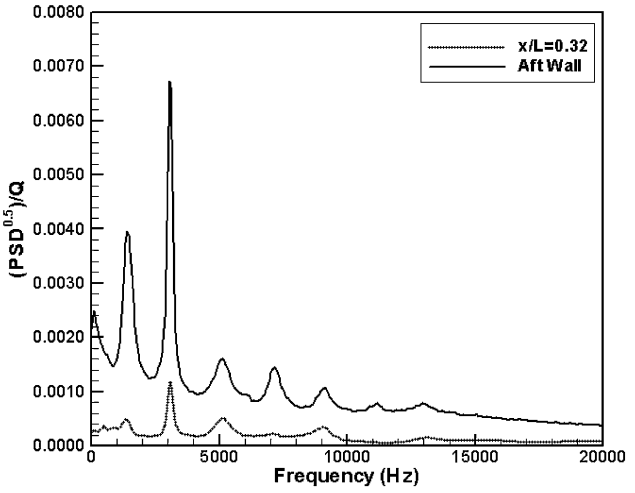

a) *L/D* = 5.6

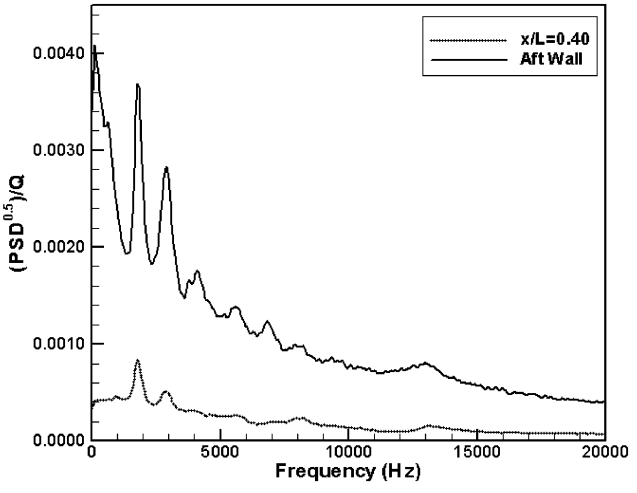

b) *L/D* = 9.0

Fig. 5 Baseline surface-pressure spectra for Mach 1.4 freestream condition.

of rms pressure in psi because the sensors on the floor of the cavity sense a mixture of hydrodynamic and acoustic pressures.

For the subsonic cases displayed in Figs. 3 and 4, one sensor was located on the aft wall, and the other was on the cavity floor at either $X/L=0.40$ or 0.25 for the 5.6 and 9.0 aspect ratios, respectively. (Note that these sensor locations are at identical x positions with respect to the cavity leading edge.) The spectral distributions of the surface pressure anywhere on the floor are quite similar regardless of the location in the cavity, although the amplitude of the surface-pressure fluctuations increases in the streamwise direction with the peak levels observed on the aft wall. The behavior observed in these plots falls into two different classes: spectra dominated by multiple peaks or dominated by a single peak. For the spectral distributions governed by multiple peaks (Figs. 3a and 4b) most of the peaks can be predicted reasonably well by either Rossiter's relationship or by solution of the wave equation for longitudinal cavity modes. Tables 1 and 2 list the calculated frequencies for the first five Rossiter modes and first four longitudinal cavity modes, respectively. The specific form of Rossiter's equation used here, along with the value of the constants, can be found in Tracy and Plentovich.[23] The tabulated longitudinal modes are calculated from solving for the normal mode frequencies of an open cavity without flow.[24] As can be observed by comparing the frequencies of the peaks in the figures to the calculated tabulated values, there is close agreement between the measured and several calculated modes. The spectral distributions governed by a single peak, Figs. 3b and 4a, result when the Rossiter mode and a longitudinal cavity mode exist at the same frequency, as has been reported originally in Rockwell and Naudascher[25] and more recently in Williams et al.[26] This can be viewed for the $L/D=9.0$ cavity with Mach 0.6 freestream condition case where the second longitudinal cavity mode is approximately equal to the fourth Rossiter mode. It is also the case for the $L/D=5.6$ aspect ratio cavity with Mach 0.75 freestream flow where the first longitudinal cavity mode is approximately equal to the second Rossiter mode. These two cases imply that it is not important which longitudinal cavity mode overlaps with a Rossiter mode.

For the Mach 1.4 freestream case (Fig. 5), the spectral plots display the aft wall sensor and one close to the center of the cavity on the floor. The presence of Rossiter modes is apparent on the aft wall sensor for both cavities. Comparing the spectra on the aft wall to the floor, one observes higher overall pressure levels on the aft wall, similar to the subsonic cases presented. In the center of the cavity floor, the second Rossiter mode is the most dominant feature. This dominance of the second mode was seen by all sensors on the cavity floor. However, near the center of the cavity (as displayed here), it is more pronounced and spectral peaks associated with the other modes, especially the first one, were not observed. Even though the other modes did not appear in the spectra, the overall pressure levels at this location were consistent with what has been previously observed and fits the overall trend of the pressure levels increasing in the streamwise direction. This trend has been observed previously and has been used to explain how the source of the cavity noise is associated with the events on the aft wall. One other trend that can be observed is that the pressure levels on the aft wall are lower for the larger cavity. This is as a result of the cavity being larger and right on the edge of transitioning to a closed cavity where the flow enters the cavity and attaches along the cavity floor.

Correlations

Because multiple sensors along the bottom of the cavity were sampled simultaneously for the Mach 1.4 runs, calculation of the cross-correlation coefficients was possible. A representation of the cross-correlation coefficients for both cavity aspect ratios is displayed in Fig. 6. This figure displays the cross-correlation coefficients for the aft wall sensor correlated with itself, three sensors along floor and one in the front wall of the cavity. These plots have been truncated to examine small time separations, that is, the first wave traveling upstream. However, their long-term behavior is best characterized as decaying oscillations. Examining the autocorrelation of the aft wall sensor (Aft Wall X Aft Wall), there are some slight differences between the different aspect ratio cavities. The most striking feature is the lack of secondary peak in the larger cavity. The time lag of this peak for the smaller aspect ratio cavity corresponds to the second Rossiter mode. The fact that it is less apparent in the larger aspect ratio implies that although there is a periodic event it is less correlated with the previous ones. Examining the cross-correlations for both cavities, the temporal behavior is similar where one can observe a wave propagating in the upstream distance at a speed just slightly greater than the local speed of sound. The trends observed in the amplitudes of the cross-correlation coefficients are also similar for the two aspect ratios, although the amplitudes for the shorter cavity are significantly greater. For the $L/D = 5.6$ cavity the correlation coefficients reduce as a function of upstream distance until about the center of the cavity, then begin to rise until it reaches a value of nearly 0.7 for the correlation between the front and aft walls of the cavity. For the $L/D = 9.0$ cavity the coefficients decrease throughout the whole cavity but finally increase to a level of approximately 0.25 for the correlation between the front and aft walls. The fact that the correlation levels between the aft wall and the front wall increase is evidence of a resonant feedback phenomena that reinforces what happens at the lip of the cavity.

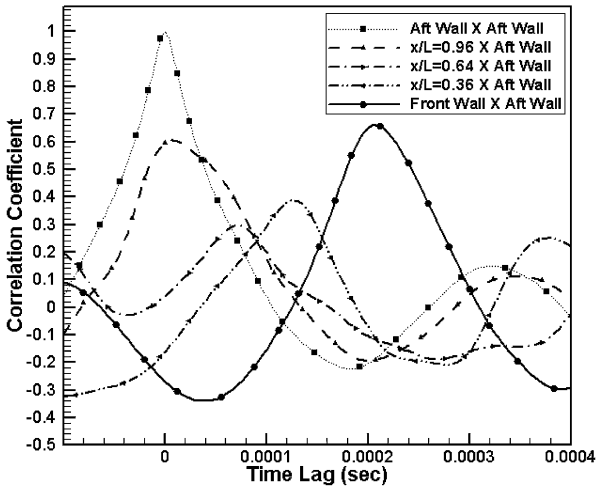

a) *L/D* = 5.6

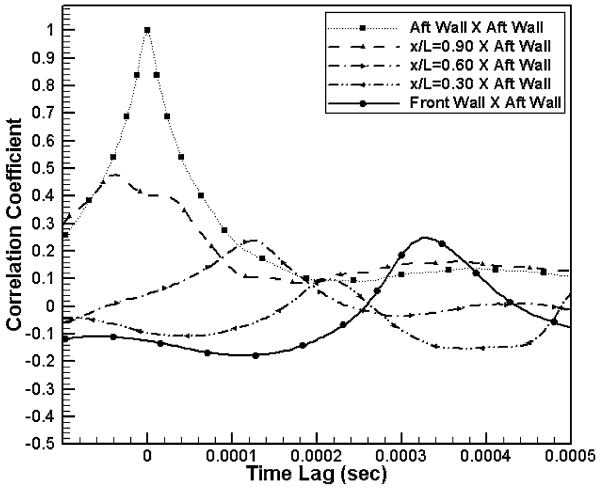

b) *L/D* = 9.0

Fig. 6 Correlation coefficients Mach 1.4.

Suppression

In the following section the results of applying devices for suppressing the pressure oscillations on the cavity floor are discussed. Specifically, two devices will be evaluated: a solid fence at the leading edge of the cavity and a rod aligned parallel to the leading edge of the cavity suspended at various heights in the incoming boundary layer.

Initial Profiles

Mach-number profiles acquired by traversing the total pressure probe in the wall normal direction at 2.92 mm downstream of the cavity lip are presented in Fig. 7. The results presented here are for the $L/D = 5.6$ cavity with Mach 0.6 freestream flow. Similar measurements were also acquired for the $L/D = 9$ cavity and freestream conditions of Mach 0.75, and the results were found to be similar to

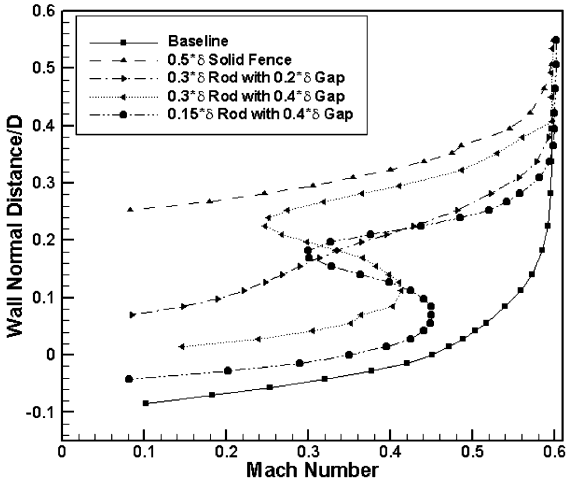

Fig. 7 Mach-number profiles at 2.92 mm downstream of cavity lip.

that described next. The calculation of Mach number was performed using the static pressure at the inlet of the test section, not from a local static-pressure measurement. The profiles presented in this figure are shown for the baseline case, a solid fence protruding 1.27 mm (half of the height of the approaching boundary layer δ) above the top plane of the cavity, a cylinder of diameter 0.76 mm ($0.3*\delta$) with gaps underneath it of 0.51 ($0.2*\delta$) and 1.02 mm ($0.4*\delta$), and a cylinder of diameter 0.38 mm ($0.15*\delta$) with a 1.02-mm gap underneath

it. All of the suppression elements at the leading edge resulted in lifting the initial shear layer into the free-stream flow with the solid fence lifting it the farthest. A fair comparison is observed between the $0.3*\delta$ cylinder with a $0.2*\delta$ gap and the solid fence because they both have the same overall penetration into the incoming boundary layer. The profile for the solid fence did not achieve the freestream value until 0.5 cavity depths above the solid wall while the profile for the cylinder with the $0.2*\delta$ gap obtained the freestream value at 0.37 D. In fact the $0.5*\delta$ solid fence lifts the initial shear layer further into the freestream than the case where the cylinder is at a higher location in the approaching boundary layer. Comparing the profiles of the 0.76-mm cylinder with the two different gaps, one observes quite different behavior. The larger gap $0.4*\delta$ has a profile that clearly shows the mean defecit of the cylinder. The smaller gap $0.2*\delta$ shows an inflection in the profile but no clear evidence of the cylinder wake. The difference in these two profiles implies that the smaller gap is too close to the wall for the flow to travel in a normal fashion underneath the cylinder and set up the normal dynamics of a cylinder in a cross flow. Profiles with the cylinder at larger separations from the wall (not shown) were similar to the one with the $0.4*\delta$ gap only with the point of maximum deficit raised. Comparison of the $0.15*\delta$ cylinder to the $0.3*\delta$ one with $0.4*\delta$ gap shows how the larger cylinder is more effective at lifting the shear layer and altering its trajectory. Profiles with other configurations were also measured, and the trends were consistent with the behavior just discussed.

Suppression with Solid Fence

In an attempt to examine the effects of raising the initial shear layer, pressure measurements from the dynamic sensors in the cavity were acquired for four different heights of the solid fence: 0.64, 1.27, 1.91, and 2.54 mm. These heights correspond to 0.25, 0.5, 0.75, and 1 boundary-layer height for the Mach 0.6 flow and 0.31, 0.62, 0.93, and 1.25 boundary-layer heights for the Mach 0.75 case. Figures 8 and 9 display the suppression in the integrated measured pressure levels for the $L/D = 5.6$ and 9.0 cavities, respectively. The ordinate on these graphs is the baseline case divided by the measured rms pressure case; therefore, values greater than one show a reduction in the overall rms pressure sensed in the cavity. The abscissa on these plots is the streamwise position in the cavity normalized by its overall length.

The level of reduction for the smaller cavity is quite different for Mach 0.60 and 0.75 (Fig. 8). For the Mach 0.6 condition the reduction reaches its maximum on the aft wall, where the overall rms pressure is reduced by factors ranging from 2 to 2.5 depending on the height of the fence. However the reduction inside the cavity was much less, implying the main effect of the spoiler, for this Mach number and aspect ratio, was to minimize the shear-layer interaction with the aft wall of the cavity. For the Mach 0.75 case fence heights

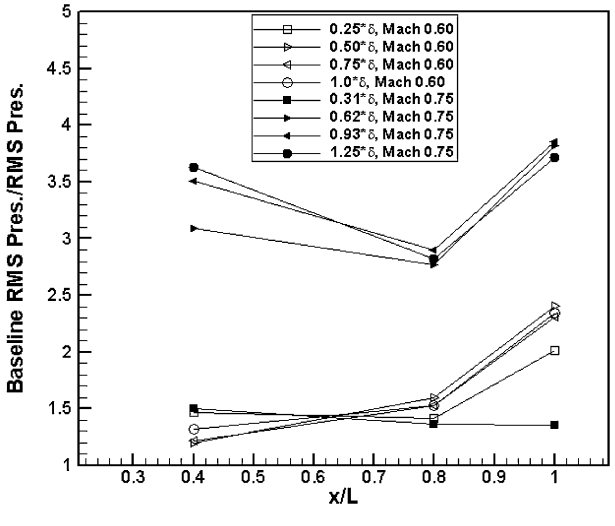

Fig. 8 Suppression with solid fence: $L/D = 5.6$.

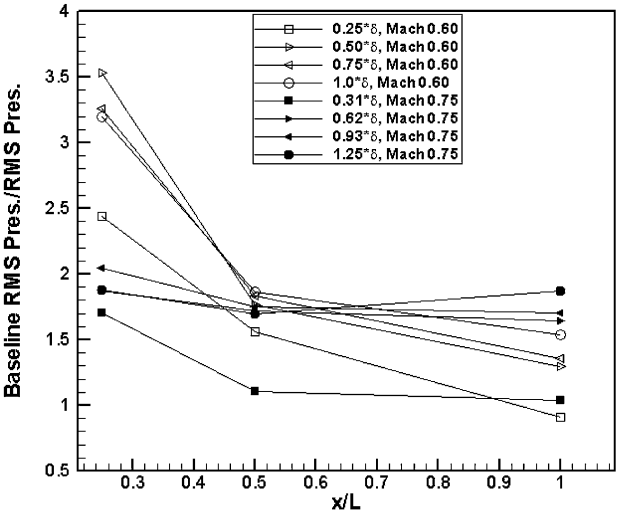

Fig. 9 Suppression with solid fence: $L/D = 9.0$.

of $0.6*\delta$ and greater produced a reduction of the pressure by factors ranging between three and four. The reductions near the center of the cavity were the largest for the highest fence, while on the aft wall of the cavity the largest corresponds to the $0.93*\delta$ fence. The results in the front half of the cavity show how the further up into the freestream the shear layer is pushed the greater the reduction. This implies that sources in the shear layer contribute to the surface pressure sensed in the front part of the cavity, and all of the surface-pressure fluctuations are not driven by the interaction of the shear layer and the aft wall. However, on the aft wall this was not the case, although the reduction only varied slightly with fence height. The $0.31*\delta$ fence height for Mach 0.75 only reduced the pressure in the cavity by factors between 1.2 and 1.5 with the greatest reduction at the leading edge of the cavity.

The behavior of the pressure reductions in the longer cavity had similar trends at both Mach 0.6 and 0.75 and were quite different from the smaller aspect ratio cavity. The largest factors of pressure reduction were always found on the foremost sensor in the cavity especially for the Mach 0.6 freestream condition. On the aft wall of the cavity, the reduction factors ranged from 1.7 to a slight augmentation of the pressure levels for the $0.25*\delta$ spoiler with Mach 0.6 flow. The trends associated with the effect of fence height for the longer cavity are reversed from those observed with the shorter cavity. Here on the aft wall of the cavity the further the fence protruded into the incoming boundary layer the greater the reduction in the pressure levels. This implies that simply lifting the shear layer to minimize its interactions with the aft wall will minimize the pressure levels on that wall.

For the three cases where the surface-pressure spectra were dominated by a single peak, the effect of the fence is noticeably better for fence height of $0.5*\delta$ and greater. This is likely caused by the shifting of the power from a single mode to multiple modes as has been observed in similar experiments using gas injection by Ukeiley et al.[27]

Suppression with Cylinder: Subsonic Flow

Figure 10 displays Mach-number profiles in the shear layer above the shorter aspect ratio cavity for the baseline and cases of a $0.3*\delta$ cylinder with gaps of $0.4*\delta$ and $0.6*\delta$ at a streamwise position of $X/L = 0.8$. As with the initial profiles, only total pressure was obtained at the measurement location, and the static pressure at the inlet to the test section was used to calculate the Mach numbers. Although the static pressure in the cavity is likely to vary from that at the inlet to the test section, the trends discussed in what follows should not differ. The wake of the cylinder that was viewed in Fig. 7 is no longer evident at this downstream location, approximately 42 cylinder diameters downstream. The difference between the suppressed case and the naturally developing cavity is clearly evident and quite pronounced. For both cylinder locations the shear layer is

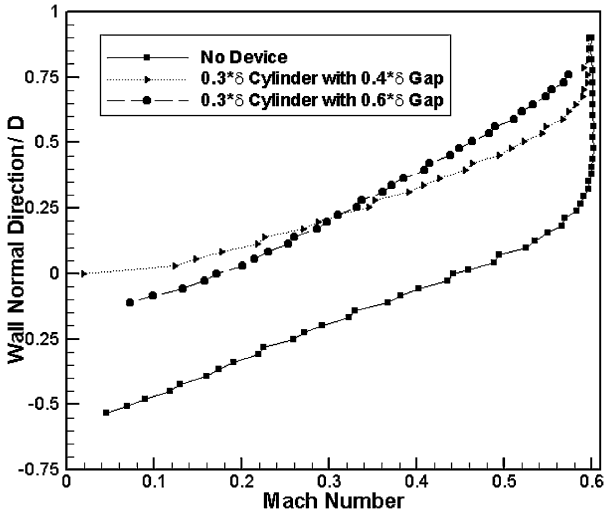

Fig. 10 Mach-number profiles at $X/L = 0.8$ and Mach 0.60.

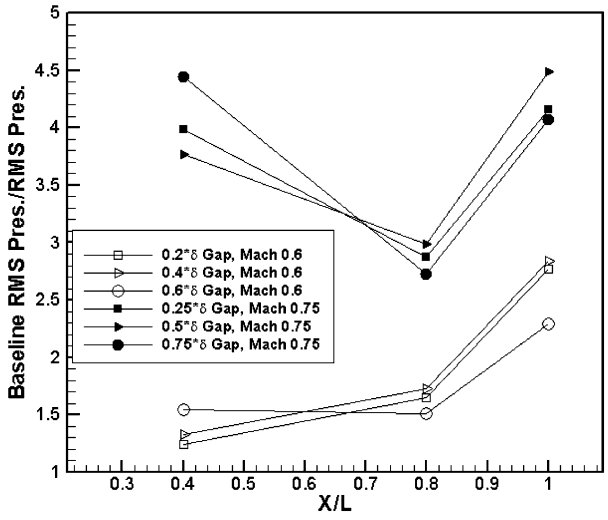

Fig. 11 Pressure reduction in $L/D = 5.6$ cavity at Mach 0.60 and Mach 0.75.

significantly higher and for the most part above the top of the cavity. The slope of the mean profile is similar for the baseline and the case where the cylinder has a $0.6*\delta$ gap. However, the case with a cylinder gap of $0.4*\delta$ has a much smaller slope. The slope of the mean profiles is related to the mean shear and thus should be a measure of the production of turbulence in the shear layer. Because the center of the shear layers for the two suppression cases is in approximately the same wall-normal location, any differences in the pressure levels between these two cases should be caused by the reduction of turbulence production in the shear layer. The behavior of the profiles at Mach 0.75 was found to be similar, although measurements were not able to be performed for the supersonic freestream case. The results observed here are consistent with simulations that were reported in Arunajatesan et al.,[20] which showed the wake of the cylinder being mixed quite rapidly with a substantial lifting of the shear layer above the top of the cavity.

Figures 11 and 12 display the reduction in the fluctuating surface pressure measured in the cavity for the 0.76-mm cylinder ($0.3*\delta$ for Mach 0.6 and $0.37*\delta$ for Mach 0.75) placed at three different heights in the approaching boundary layer. Plotted in these figures is the baseline rms pressure normalized by the rms pressure as a function of downstream location in the cavity for the three gap heights. In each figure the open symbols represent Mach 0.6, and the filled symbols represent Mach 0.75 freestream conditions. For both cavity aspect ratios there is a general increase in the baseline pressure level in the streamwise direction for the baseline cavity as was discussed earlier and has been reported in many previous studies. The cylinder with gap heights approximately $0.5*\delta$ led to the lowest pressure levels in the cavity for both aspect ratios at both freestream Mach numbers, although the reduced levels are all quite similar. This result is consistent with that of Smith et al.[19] because this location is the one where the cylinder is nearly aligned with the top of the boundary layer. If one considers that the mean shear was slightly less for the $0.4*\delta$ gap, it makes sense to think that sources driving some of the fluctuating surface-pressure levels are driven by the turbulence in the shear layer. Because the suppressed values are nominally the same and the baseline value for the Mach 0.75 is significantly greater than the Mach 0.6 case, the ratio of suppressed to baseline has the same trend as the cases with the spoiler at this aspect ratio, that is, the level of suppression is much more significant for the Mach 0.75 case. The reduction factor observed for the Mach 0.75 case is 4.5 on the aft wall showing the cylinder to be slightly more effective than the solid fence. The trend observed for the larger aspect ratio cavity with the solid fence of the suppression level not being dependent on Mach number was also observed with the cylinders. The larger cavity has a more pronounced difference between the 1.02- and 1.52-mm gaps.

Although not explicitly discussed before a small study to examine the effect of the cylinder diameter was performed with freestream Mach numbers of 0.60 and 0.75. It was found that the 0.76-mm cylinder provided the greatest levels of suppression; however, the trends observed were similar for all diameters examined. These results were consistent with those reported by Smith et al.,[19] where

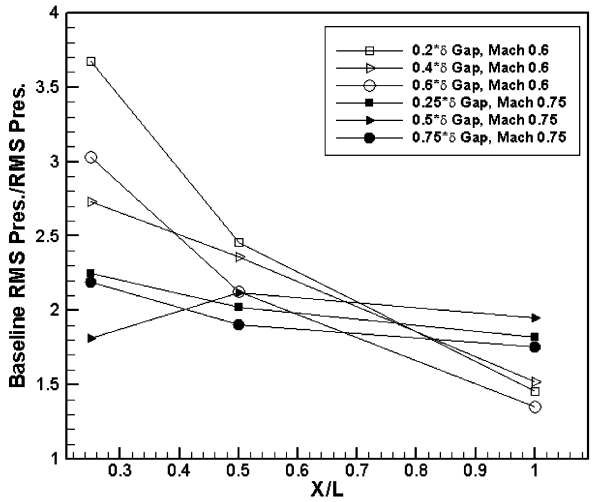

Fig. 12 Pressure reduction in $L/D = 9.0$ cavity at Mach 0.60 and Mach 0.75.

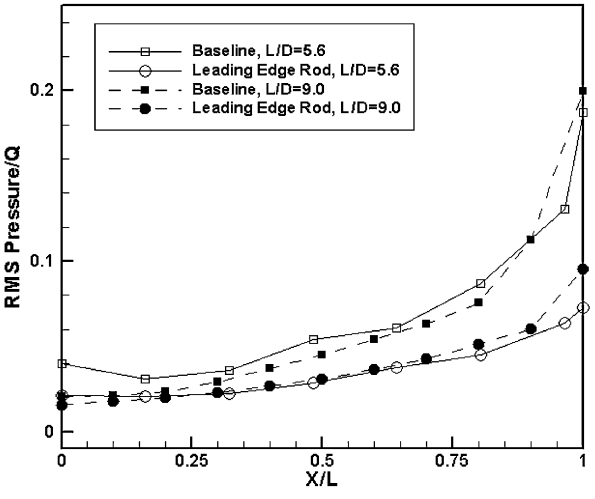

Fig. 13 Suppression in Mach 1.4 with rod.

it was determined that in general the larger the diameter the more effective the suppression is.

Suppression with Cylinder: Supersonic Flow

Unlike the subsonic cases both aspect ratios behave similarly and have nominally the same normalized pressure levels. This is because of the increased range of aspect ratios that act in a transitional manner as the Mach number is increased, as reported in Tracy and Plentovich,[23] that is, both cavities behave in a open fashion. For both aspect ratios the pressure level reductions inside the cavity are not that large in the front half of the cavity, but they increase throughout the cavity and are quite large on the aft wall. On the aft wall the pressure levels are reduced by approximately a factor of two, which is on the order of what was found for the subsonic cases. The reductions in the front part of the cavity were approximately the same. Also, the shedding frequency of the cylinder should be approximately 130 kHz, based on the frestream velocity and a Strouhal number of 0.2, which is larger than the maximum resolved frequencies in the spectra that were integrated to obtain the values in Fig. 13. Therefore, one might expect the results to be slightly worse if the spectra could resolve the shedding. However, it is highly unlikely that the flow would be able to respond to frequencies that high and would most likely damp them out. This is based on the results of Tam,[28] where through a hydrodynamic stability analysis it was shown that for a compressible single stream mixing layer the unstable frequencies resided in a range of Strouhal numbers up to approrimately 0.35. If one estimates the Strouhal number here using an estimate for the initial momentum thickness, one finds values atleast one order of magnitude larger.

Figure 14 show comparisons of the narrowband spectra for the baseline vs suppressed cases for the $L/D = 5.6$ cavity with Mach 1.4 freestream flow. On the front wall of the cavity, Fig. 14a indicates that the reduction of the pressure signal is mostly obtained by reducing the levels of the peaks and little is done to the broadband levels. In the downstream end of the cavity (Figs. 14b and 14c), the suppression element was able to reduce the levels of the peak as

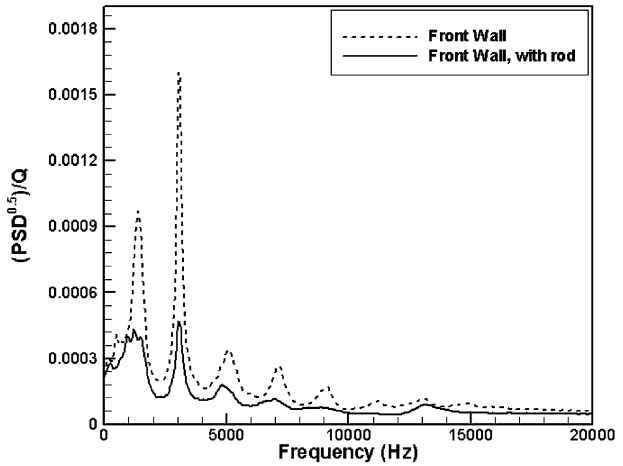

a) Front wall

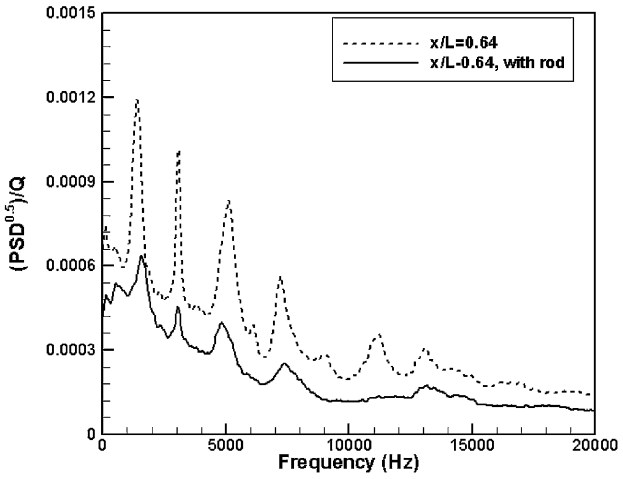

b) $x/L = 0.64$

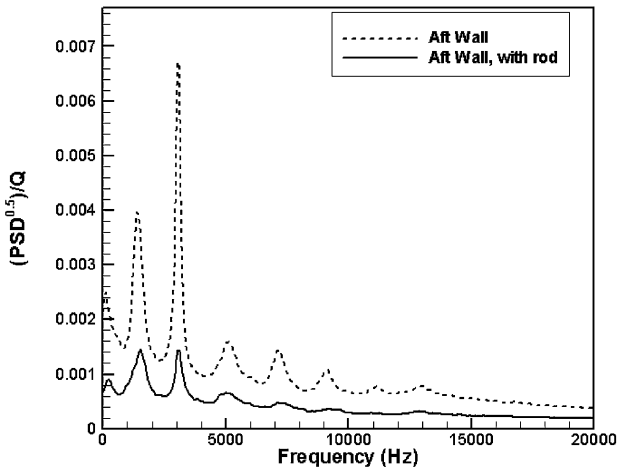

c) Aft wall

Fig. 14 Narrowband spectra of suppression in Mach 1.4 with rod.

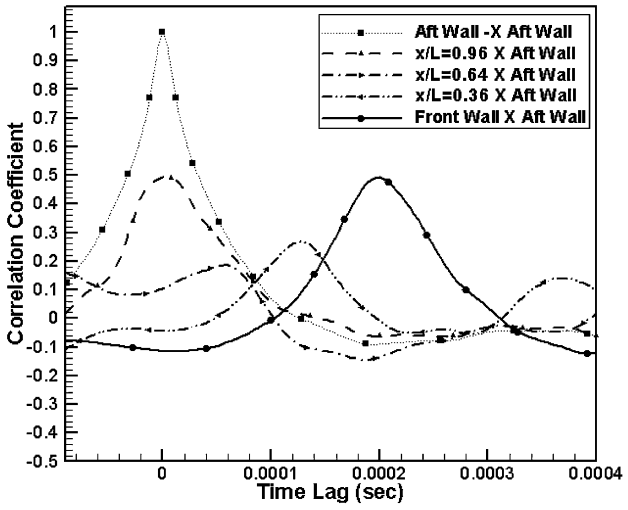

a)

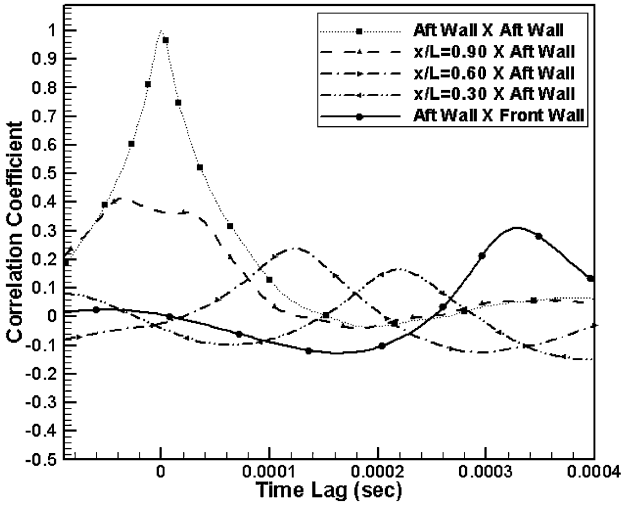

b)

Fig. 15 Correlation coefficients of Mach 1.4: a) $L/D = 5.6$ and b) $L/D = 9.0$ with rod.

well as generally reduce the broadband levels. The persistence of the tones in the spectra imply that the dynamics of the shear layer and the aft wall still persist in some degree setting up the resonant phenomena. This reduction of the peak tonal levels along with the broadband levels in the aft part of the cavity was observed in both the subsonic and supersonic cases.

Figure 15 displays the correlation coefficients from the $L/D = 5.6$ and 9.0 cavity and Mach 1.4 freestream flow with the leading-edge cylinder for the same sensor locations as Fig. 6. Comparing these plots to the uncontrolled cases, one observes that the time dependence has not been altered while the amplitudes have been significantly reduced. If one assumes that amplitude values are representative of the strength of the feedback modes, then this implies a lessening of the resonant feedback.

Conclusions

The effects of two leading-edge suppression devices were studied to develop an understanding of how they reduce the fluctuating pressure loads inside an open cavity. Dynamic pressure transducers were used to measure the fluctuating surface pressures that were analyzed for cavities with length-to-depth aspect ratios of 5.6 and 9.0 and subjected to freestream Mach numbers of 0.6, 0.75, and 1.4. The leading-edge devices studied here were a solid fence and cylindrical rod suspended in the approaching boundary layer parallel to the leading edge of the cavity.

Baseline measurements of cavities with no suppression devices showed good agreement with historical data in terms of amplitude and Rossiter's equation in terms of peak frequencies. Examination of cross correlations between the aft wall and sensor on the floor of the cavity showed a wave front propagating upstream. The existence of this event is consistent with previously obtained optical measurements and was interpreted as the wave being carried upstream by the reverse flow in the bottom of the cavity.

Although the source of noise in a cavity has long been linked to the interaction of the shear layer with aft wall, simply lifting the shear layer higher into the freestream did not minimize the fluctuating pressures inside the cavity. This was verified through two different methods. Mach-number profiles measured just downstream of the leading edge of the cavity showed that the solid fence was the most effective at lifting the initial shear layer formed above the cavity into the freestream flow. However, the cylinders suspended in the boundary layer at the leading edge of the cavity produced lower fluctuating pressure levels in the cavity. Similarly, raising the height of the leading-edge fence did not always result in lower fluctuating pressure levels in the cavity. For the smaller-aspect-ratio cavity studied, there was very little difference in the pressure levels in the cavity once the fence extended beyond a third of the boundary-layer height. For the larger aspect ratio the fluctuating pressures on the aft wall were reduced as the fence protruded higher into the boundary layer, but the reduction in the front of the cavity was decreased as the fence was moved more into the flow. This implies that for the transitional cavity $L/D = 9$ in subsonic flow the fluctuating pressure on the aft wall is driven by the shear-layer interactions with the aft wall. However, in the front of the cavity pressures are driven by a combination of noise produced in the shear layer locally and noise fed upstream from the back of the cavity.

Suspending a cylinder at the leading edge of the cavity was shown to be an effective way to reduce the fluctuating pressure load inside the cavity for both subsonic and supersonic freestream conditions. It was found that the maximum reduction occurred when the cylinder was suspended such that the top of it was near the top of the boundary layer, yet still in the boundary layer, and the gap underneath it was large enough so that the flow could establish a wake pattern. For subsonic freestream conditions the behavior was quite different for the two aspect ratios, while for supersonic freestream conditions both aspect ratios behaved similarly with a maximum reduction of approximately 50% on the aft wall. Examination of narrowband spectra showed that in the back half of the cavity the reduction was obtained by reducing the peak amplitudes as well as a general reduction of the broadband levels. Mach-number profiles near the trailing edge of the cavity showed how the suppression devices raised the shear layer along with altering the mean shear. The reduced mean shear was shown to be more effective at reducing the fluctuating pressure levels for the larger aspect ratio cavity at Mach 0.75 freestream conditions, although it seemed to have some effect for all of the subsonic cases examined. Cross correlations of the sensors in the cavity with the aft wall sensor suggest that the amplitude of the upstream traveling wave along the floor of the cavity was reduced slightly, thereby implying that the strength of the resonant features of the cavity were reduced in conjunction with the broadband reductions for the suppressed case.

The results presented in this work imply that the effectiveness of the cylinder to reduce the pressure loads inside of the cavity comes from the lifting of the shear layer. However, a recent study reported in Stanek et al.[29] studied similar configurations of suspending rods in the approaching boundary layer and concentrated on whether there was high-frequency shedding from the cylinder. Their conclusion was that it is the shedding that interacts with the shear layer above the cavity, thereby altering it in a manner that reduces the fluctuating pressure inside the cavity. To better define the mechanisms for reducing pressure loads inside the cavity with leading-edge cylinders, a study is currently under way to acquire detailed flow measurements of the cavity shear layer.

Acknowledgments

This work was conducted with support from the U.S. Air Force Office of Scientific Research, in grants monitored by both S. Walker and J. Schmisseur. The authors acknowledge the Aeronautics Department at the U. S. Air Force Academy for the use of the Trisonic Tunnel, especially Maj. Rhett Jefferies and Larry Lamblin. The authors also acknowledge the support of our colleagues at the Jet Noise Laboratory at NASA Langley Research Center who have loaned us the duct we are running at the National Center for Physical Acoustics.

References

[1]Krishnamurty, K., "Acoustic Radiation from Two-Dimensional Rectangular Cutouts in Aerodynamic Surfaces," NACA TN 3487, Aug. 1955.

[2]Roshko, A., "Some Measurements of Flow in a Rectangular Cutout," NACA TN 3488, Aug. 1955.

[3]Rossiter, J. E., "Wind Tunnel Experiement on the Flow over Rectangular Cavities at Subsonic and Transonic Speeds," Ministry of Aviation, Aeronautical Research Council 3438, Oct. 1964.

[4]Heller, H. H., and Bliss, D. B., "Aerodynamically Induced Pressure Oscillations in Cavities—Physical Mechanisms and Suppression Concepts," Flight Dynamics Lab., AFFDL TR-74-133, Feb. 1975.

[5]Heller, H., and Delfs, J., "Cavity Pressure Oscillations: The Generating Mechanisms Visualized," *Journal of Sound and Vibration*, Vol. 196, No. 2, 1996, pp. 248–252.

[6]Clark, R. L., "Weapons Bay Turbulence Reduction Techniques," Flight Dynamics Lab., AFFDL TM-75-147-FXM, Dec. 1975.

[7]Shaw, L. L., "Suppresion of Aerodynamically Induced Cavity Pressure Oscillations," Flight Dynamics Lab., AFFDL TR-79-3119, Nov. 1979.

[8]Dix, R. E., and Butler, C., "Cavity Aeroacoustics," U.S. Air Force, AFATL-TP-90-08, June 1990.

[9]Dix, R. E., and Bauer, R. C., "Experimental and Predicted Acoustic Amplitudes in a Rectangular Cavity," AIAA Paper 2000-0472, Jan. 2000.

[10]Kegerise, K. A., Spina, E. F., and Cattafesta, L. N., "An Experimental Investigation Flow-Induced Cavity Oscillations," AIAA Paper 99-3705, June 1999.

[11]Cattafesta, L. N., Garg, S., Kegerise, K. A., and Jones, G. S., "Experiments on Compressible Flow-Induced Cavity Oscillations," AIAA Paper 98-2912, June 1998.

[12]Shaw, L. L., and Mcgrath, S., "Weapons Bay Acoustics—Passive or Active Control," AIAA Paper 96-1617, April 1996.

[13]Sarno, R. L., and Franke, M. E., "Suppression of Flow-Induced Pressure Oscillations in Cavities," *Journal of Aircraft*, Vol. 31, No. 1, 1994, pp. 90–96.

[14]Shaw, L., and Northcraft, S., "Closed Loop Active Control for Cavity Acoustics," AIAA Paper 99-1902, June 1999.

[15]Williams, D. R., Fabris, D., Iwanski, K., and Morrow, J., "Closed Loop Control in Cavities with Unsteady Bleed Forcing," AIAA Paper 2000-0470, Jan. 2000.

[16]Cattafesta, L. N., Shukla, D., Garg, D. S. S., and Ross, J. A., "Development of an Adaptive Weapons-Bay Suppresion Systems," AIAA Paper 99-1901, June 1999.

[17]Stanek, M. J., Raman, G., Kibens, V., Ross, J. A., Odedra, J., and Peto, J. W., "Control of Cavity Resonance Through Very High Frequency Forcing," AIAA Paper 2000-1905, June 2000.

[18]Mcgrath, S., and Shaw, L., "Active Control of Shallow Cavity Acoustic Resonance," AIAA Paper 96-1949, June 1996.
[19]Smith, B., Welteren, T., Maines, B., Shaw, L., Stanek, M., and Grove, J., "Weapons Bay Acoustic Suppression from Rod Spoilers," AIAA Paper 2002-0662, Jan. 2002.
[20]Arunajatesan, S., Shipman, J., and Sinha, N., "Hybrid Rans-LES Simulation of Cavity Flow Fields with Control," AIAA Paper 2002-1130, Jan. 2002.
[21]Sinha, N., Arunajatesan, S., and Seiner, J., "Computational and Experimental Investigations of Cavity Attenuation Using High Frequency Control," AIAA Paper 2002-2403, May 2002.
[22]Ponton, M., Seiner, J., Ukeiley, L., and Jansen, B., "A New Anechoic Chamber Design for Testing High-Temperature Jet Flows," AIAA Paper 2001-2190, May 2001.
[23]Tracy, M. B., and Plentovich, E. B., "Cavity Unsteady-Pressure Measurements at Subsonic and Transonic Speeds," NASA TP 3669, Dec. 1997.
[24]Kegerise, K. A., "An Experimental Investigation of Flow Induced Cavity Oscillations," Ph.D. Dissertation, Dept. of Mechanical Engineering, Syracuse Univ., Syracuse, NY, Aug. 1999.
[25]Rockwell, D., and Naudascher, E., "Review of Self-Sustaining Oscillations of Flow Past Cavities," *Journal of Fluids Engineering*, Vol. 100, 1978, pp. 152–165.
[26]Williams, D. R., Fabris, D., and Morrow, J., "Experiments on Controlling Multiple Acoustic Modes in Cavities," AIAA Paper 2000-1903, June 2000.
[27]Ukeiley, L., Ponton, M., Seiner, J., and Jansen, B., "Suppression of Pressure Loads in Resonating Cavities Through Blowing," AIAA Paper 2003-0181, Jan. 2003.
[28]Tam, C. K. W., "Excitation of Instability Wave in a Two-Dimensional Shear Layer by Sound," *Journal of Fluid Mechanics*, Vol. 89, No. 2, 1978, pp. 357–371.
[29]Stanek, M. J., Ross, J. A., Odedra, J., and Peto, J. W., "High Frequency Acoustic Suppression—The Mystery of the Rod-in-Crossflow Revealed," AIAA Paper 2003-0007, Jan. 2003.

H. M. Atassi
Associate Editor